

Short Communication

Composites of Electrochemically Reduced Graphene Oxide and Polythiophene and Their Application in Supercapacitors

F. Ibáñez-Marín^{2,3}, C. Morales-Verdejo¹, M.B. Camarada^{4,*}

¹ Centro de Genómica y Bioinformática, Facultad de Ciencias Universidad Mayor, Santiago, Chile

² Universidad Bernardo OHiggins, Departamento de Ciencias Químicas y Biológicas & Escuela de Kinesiología, General Gana 1702, Santiago, Chile.

³ Centro Integrativo de Biología y Química Aplicada (CIBQA), Universidad Bernardo OHiggins, General Gana 1702, Santiago, Chile

⁴ Centro de Nanotecnología Aplicada, Facultad de Ciencias, Universidad Mayor, Chile

*E-mail: maria.camarada@umayor.cl

Received: 12 August 2017 / Accepted: 17 October 2017 / Published: 12 November 2017

Composite films consisting of polythiophene (PTh) and graphene oxide (GO) were synthesized by electrochemical polymerization. Consequently, the GO was reduced via cyclic voltammetry to form a reduced composite (PTh/rGO), which presented higher conductivity than PTh. Specific capacitance values were calculated from galvanostatic charge-discharge profiles. At a current density of $0.5 \text{ A} \cdot \text{g}^{-1}$, the specific capacitance of PTh/rGO presented a good value ($318 \text{ A} \cdot \text{g}^{-1}$). However, its behavior was distant from a typical supercapacitor, indicative of a low reversibility during the charge-discharge processes and poor capability as supercapacitor material. Moreover, its stability diminished considerably after repetitive cycling. Experimental conditions of synthesis of PTh/rGO require to be optimized for the application of the composite as electrode material in supercapacitors.

Keywords: polythiophene, graphene oxide, supercapacitors

1. INTRODUCTION

Future energy demands strongly require inexpensive, flexible and sustainable storage systems with large energy and power density [1,2]. During the last years, electrochemical supercapacitors have raised as promising energy storage devices, due to their higher power density, faster charging-discharging processes, and higher energy storage compared to the Li-ion batteries [3,4]. In general, depending on the energy storage mechanisms, supercapacitors can be can be classified into two general categories: electrical double layer capacitors (EDLCs) and pseudo capacitors (PCs) [5]. EDLCs store electrical energy by using the electrical double layer capacitance via reversible ion absorption at the electrode/electrolyte interface. In contrast, PCs are related to fast reversible faradaic reactions at the

surface of electroactive materials [6,7]. EDLCs have energy densities and specific capacitances values close to a conventional capacitor due to the nature of electrode materials and the limited surface area. On the other hand, PCs have higher energy density and a fast loss of power density at the cost of a shorter life cycle [8]. They can store greater charge than EDLCs because of the smaller charge separation at the electrode/electrolyte interface and the pseudocapacitance resulting from faradaic reactions at the interface. Nevertheless, the use of PCs is usually restricted to low working voltages. They also show stability issues and unsatisfactory high/rate capabilities, arising from low conductivities of electrode materials [9]. Therefore, the real challenge in the electrochemical performance of supercapacitors is to promote their energy density and preserve their high power capability and long cycle life [10,11] through the rational selection of electrode materials and design of high surface area morphology [12].

Many carbon materials have been employed for EDLCs because of their high surface area and superior electric double layer capacitance, which can store charge by ion adsorption/desorption at the interface between electrode and electrolyte, leading to enhanced electrochemical performance [13-15]. Among these materials, graphene (GR), a single layer of sp^2 -bonded carbon atoms, is one of the most attractive because of its excellent electrical and thermal conductivity, electrochemical stability and mechanical properties [16,17]. However, up to date graphene remains as a relatively expensive material because of the absence of large-scale production technology. Graphene oxide (GO), which can be easily synthesized from graphite at lower cost, appears as a viable option. GO can be typically reduced (rGO) with hydrazine, hydrothermal reduction, high temperature treatment and laser-writing method [18,19].

Recently, graphene derived materials have been combined with conducting polymers in order to improve the performance of supercapacitor electrodes through the synergistic effect of EDLC capacitance and pseudo-capacitance. The resulting materials usually show better electrochemical properties than their pure conducting polymer counterparts, such as a higher conductivity and increased stability during the charge-discharge process [20,21]. Polythiophene (PTh) is considered as one of the most promising conducting polymers because of its low cost, high environmental stability and good electrical conductivity. *Laforge* and co-workers performed the first known study using PTh as a supercapacitor, reporting a specific storage level of $110 \text{ F} \cdot \text{g}^{-1}$ [22]. Since then, several compounds have been applied to improve the thermal and electrical conductivities of PTh [23,24]. To date, most of the explored GR/PTh composites have been synthesized via traditional chemical polymerization. *Zhao et al.* reported graphene nanosheet/PTh composites, which presented characteristics of a semiconductor. However, the authors did not characterize electrochemically their use in energy storage applications [25]. In 2011, *Alvi et al.* explored the use of a GR/PTh composite as supercapacitor [26], reporting a specific capacitance of $176 \text{ F} \cdot \text{g}^{-1}$. *Yadav* and coworkers, reported the covalent grafting of GO with PTh, and its subsequently reduction. The PTh/rGO composite presented a maximum capacitance of $230 \text{ F} \cdot \text{g}^{-1}$ at $1 \text{ mV} \cdot \text{s}^{-1}$ and, most significant, 100% cycling retention after 5000 cycles [27]. More recently, our group performed a study related to the chemical synthesis of GR/PTh composites with different composition ratios. The composite material with 50% PTh presented the highest capacitance, with a value of $365 \text{ F} \cdot \text{g}^{-1}$ at $1 \text{ A} \cdot \text{g}^{-1}$ [28].

Traditional chemical polymerization is the most common method used for preparing composites of conducting polymers and graphene materials [29]. The reaction is usually carried out in a graphene oxide dispersion with the monomer, which is polymerized by the use of an oxidizing agent. The GO can be subsequently reduced to graphene by the use of a reducing agent like hydrazine [30] or borohydride [31]. In comparison, electrochemical polymerization offers a quick, safe and clean synthesis method. The electrochemical perturbation applied to the system results in the direct coating of the working electrode with a composite film, with no need of oxidizing agents or annexed chemical procedures. Additionally, graphene oxide can be electrochemically reduced in a rapid manner [32,33].

In this work, we report the *in situ* synthesis of PTh and rGO composite using electrochemical methodologies, rather than tradition chemical polymerization and reduction. To the best of our knowledge, this reduction method has not been previously used for PTh–rGO composite films. This technique allows the direct and simple preparation of composites in one-step without polymeric binders or covalent modifications. The reduced PTh/rGO composite exhibited superior electrical conductivity than PTh and PTh/GO. The supercapacitance property of PTh/rGO was characterized and compared to the other synthesized materials. PTh/rGO presented low stability after cycling, being not suitable for use as an electrode material for supercapacitors.

2. EXPERIMENTAL DETAILS

2.1. Reagents

Reagents were of analytical grade or the highest commercially available purity. Graphite, and KCl were purchased from Merck. Thiophene monomer was purchased from Sigma Aldrich. Aqueous solutions used in electrochemical measurements were prepared with ultrapure water of resistivity not less than 18 M Ω cm (Milli-Q, USA). Anhydrous acetonitrile was used as solvent for the preparation of the polythiophene and polythiophene-graphene oxide (PTh/GO) composite.

2.2. Synthesis and characterization of graphene oxide (GO)

Graphene oxide was synthesized *via* Hummers' method with some modifications [34]. Briefly, 4 g of graphite powder were dissolved with vigorous stirring in 10 mL of H₂SO₄ at 90 °C and oxidized using a combination of 2 g of K₂S₂O₈ and 2 g of P₂O₅. The stirring continued for four more hours at a temperature of 80 °C. The solution was then diluted with 500 mL of Milli-Q water. After dilution, the solution was stirred overnight. The pre-oxidized graphite was then filtered and washed with deionized water until a neutral pH was achieved, and then dried at room temperature overnight. This powder was then subjected to further oxidation with 92 mL of H₂SO₄ and 12 g of potassium permanganate (KMnO₄) in an ice bath solution. The mixture was stirred for 2 more hours at 35 °C. After this, 184 mL of Milli-Q water were added to the mixture. The reaction was terminated by the addition of 10 mL of H₂O₂ and 560 mL of Milli-Q water to reduce the manganese in the solution. The color of the mixture changed to bright yellow and the mixture was then stirred overnight. The precipitate was centrifuged at

3000 rpm and washed with water until reaching a neutral pH. Finally, the obtained GO was filtered and dried under vacuum at 40°C for 24 h to avoid decomposition. Fourier transform infrared spectroscopy (FTIR) spectra were measured using a Jasco FT/IR 4100 spectrometer in the frequency range 500 – 4000 cm^{-1} , on preparing a KBr pellet. UV-visible spectra were recorded with a Jasco V-630 UV-visible spectrophotometer. All measurements were taken at room temperature. Typical signals for graphene oxide were identified by both techniques, confirming the effective synthesis of GO.

2.3. Electrochemical methods and characterization

A CH Instruments (CHI 760E) potentiostat/galvanostat electrochemical workstation was used to measure the electrochemical properties of the samples at ambient temperature (20 °C). A conventional three-compartment cell was employed throughout the work. A platinum disk electrode (2 mm diameter) was used as working electrode. The counter electrode was a coiled Pt wire of large area, separated from the electrolytic solution by a sintered glass frit. Prior to each experiment, the working electrode was polished to a mirror finish with an aqueous alumina slurry (particle size 0.3 and 0.05 micron) on micro-cloth pads, rinsed thoroughly with water and dried. All potentials are referred to a Ag/AgCl (KCl, 1 M) electrode. Each working solution was purged with high purity argon for 15 min prior to each experiment and a lower flow was maintained over the solution during the measurements. Tetrabutylammonium hexafluorophosphate ($\text{Bu}_4\text{N}\cdot\text{PF}_6$) was dried at 110 °C and kept into a dryer until used as supporting electrolyte. Acetonitrile was dried with phosphorus pentoxide under a N_2 atmosphere reflux. The PTh film was synthesized at 1.9 V on a platinum electrode from a solution of thiophene monomer (0.03 M) and supporting electrolyte ($\text{Bu}_4\text{N}\cdot\text{PF}_6$ 0.1 M) in dried acetonitrile. PTh/GO film was obtained at the same conditions, but adding GO to the solution (1 $\text{mg}\cdot\text{ml}^{-1}$). PTh/GO composites were reduced to PTh/rGO using cyclic voltammetry in KCl aqueous solution (1 M) at a scan rate of 100 $\text{mV}\cdot\text{s}^{-1}$ between -1.2 and 0.0 V. The final deposits were weighted at a microbalance in order to perform the charge-discharge characterization. Cyclic voltammetry profiles of characterization were carried out in 1 M KCl, between -0.2 and 0.8 V at a scan rate of 50 $\text{mV}\cdot\text{s}^{-1}$. Galvanostatic charge-discharge profiles were measured in KCl 1 M, at a current density of 0.1 and 0.5 $\text{A}\cdot\text{g}^{-1}$. Electrochemical impedance spectroscopy (EIS) was performed at AC voltage amplitude of 0.01 V and a frequency range from 0.1 Hz to 1000 kHz at open circuit potential.

3. RESULTS AND DISCUSSION

3.1. Electropolymerization and capacitance properties of PTh, PTh/GO and PTh/rGO

The PTh and PTh/GO films were obtained through chronoamperometry on a platinum electrode. It has been previously reported that water interferes in the formation of the conducting polymers. Electrochemical synthesis of films in aqueous electrolytes results in lower conductivity compared to those obtained from anhydrous conditions [35]. In the specific case of PTh, water even at

low levels, has a negative and critical effect in the film forming electrodeposition, modifying the radical polymerization mechanism [36,37]. Therefore, PTh film was synthesized by chronoamperometry of a solution of thiophene monomer (0.03 M) and supporting electrolyte ($\text{Bu}_4\text{N}\cdot\text{PF}_6$ 0.1 M) in dried acetonitrile at 1.9 V (Figure 1). The PTh/GO was obtained at the same conditions but adding GO to the solution ($1 \text{ mg}\cdot\text{ml}^{-1}$).

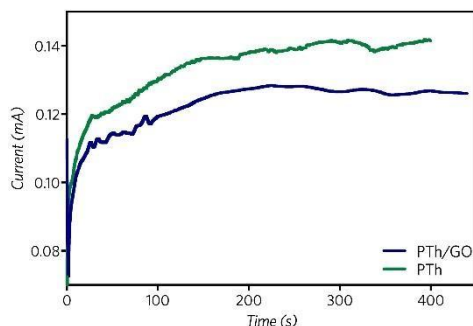


Figure 1. Chronoamperometric responses for the electrochemical formation of PTh in anhydrous acetonitrile, 0.03 M thiophene monomer and $\text{Bu}_4\text{N}\cdot\text{PF}_6$ 0.1 M, and PTh/GO composite on a platinum electrode.

In the case of PTh/GO, electropolymerization time was selected to match the final charge of the deposited PTh. The difference in the profiles is related to the incorporation of GO to the PTh network in order to maintain the electrical neutrality. The obtained films were weighted at a microbalance in order to perform the charge-discharge characterization.

The reduction of GO in the PTh/GO composite was achieved by electrochemical methods, scanning the potential from -1.2 to 0.0 V in KCl aqueous solution (1 M) at a scan rate of $100 \text{ mV}\cdot\text{s}^{-1}$. As Figure 2 shows, the reduction of GO in the PTh/GO composite appeared approximately at -0.85 V in the first scan. No peaks associated to a reduction process were detected during the second cycle.

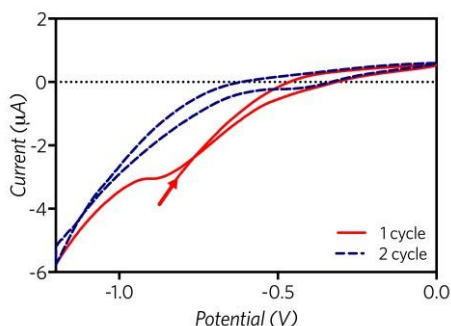


Figure 2. Cyclic voltammogram of the reduction of PTh/GO in KCl (1 M), at a scan rate of $100 \text{ mV}\cdot\text{s}^{-1}$.

Graphene oxide has hydroxyl and carboxylic groups [38] on the surface that can be reduced. After the first cycle, the GO present in the PTh/GO composite, was reduced electrochemically to rGO.

To get insights about the performance of the synthesized films, cyclic voltammetry responses of PTh, PTh/GO and PTh/rGO were recorded in KCl 1M, between -0.2 and 0.8 V at $50 \text{ mV} \cdot \text{s}^{-1}$, as Figure 3 depicts. Ideal capacitors present a rectangular symmetric current–potential characteristic. However, the synthesized PTh/rGO film deviated from this shape, which indicates the formation of a poor efficient electrochemical double layer capacitor with low charge propagation. PTh and PTh/GO exhibited a form closer to the rectangular shape.

The larger area of the curve of the reduced film is indicative of a larger capacitance in comparison to the PTh and PTh/GO films. No peaks associated to pseudofaradaic reactions were detected and thus, the activity of the PTh-rGO composite is related to the pure interaction between the charged electrode surface and ions.

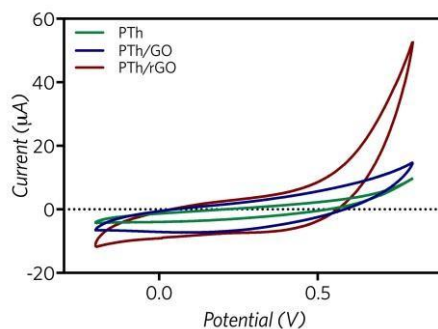


Figure 3. Cyclic voltammograms of the response of PTh, PTh/GO and PTh/rGO films on a platinum electrode in KCl 1 M at a scan rate of $50 \text{ mV} \cdot \text{s}^{-1}$.

Specific capacitance (C) of a single electrode in a three electrode system can be calculated by galvanostatic charge-discharge curves, applying the following equation [39,40]:

$$C = \frac{i \Delta t}{m \Delta V}$$

where i (A) is the discharge current, Δt (s) is the discharge time, m (g) is the mass of the active electrode material and ΔV (V) is the voltage range. In this work, a current density of 0.1 and $0.5 \text{ A} \cdot \text{g}^{-1}$ was applied in order to measure the charge-discharge curves, while the mass of the films was estimated by the use of a microbalance. The specific capacitances for the modified electrodes are summarized in Figure 4. At both current densities, the specific capacitance of PTh can be enhanced in more than 60% by the inclusion of GO. After its reduction, the capacitance increases even more, presenting improved C values in comparison to PTh and PTh/GO. This higher specific capacitance can be attributed to the larger conductivity of the reduced graphene oxide and superior surface area. However, in the case of PTh/rGO, the charge-discharge profiles exhibited an asymmetric triangular shape with a non-linear potential-time relationship, indicative of a low reversibility during the charge-discharge process and poor capability as supercapacitor material.

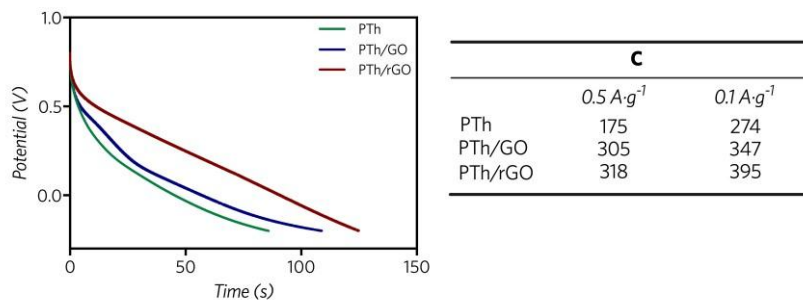


Figure 4. Discharge curves of the synthesized materials at a current density of 0.1 A g^{-1} and specific capacitance values of the electrodes ($\text{F} \cdot \text{g}^{-1}$) at different current densities.

The specific capacitance of PTh/rGO at $0.5 \text{ A} \cdot \text{g}^{-1}$ ($318 \text{ A} \cdot \text{g}^{-1}$) presents a good value, however its behavior is far from a typical supercapacitor. Previous C obtained at the same conditions report $180 \text{ F} \cdot \text{g}^{-1}$ for 3D N-doped graphene–carbon nanotubes networks [41], $287 \text{ F} \cdot \text{g}^{-1}$ for pyrolyzed GO/resorcinol–formaldehyde resin composite [42], $275 \text{ F} \cdot \text{g}^{-1}$ for S-doped graphene oxide hybrid nanosheets by *in situ*-polymerization of a thiophene derivative (thiophene-2,5- diyl)-co-(benzylidene) [43] and $740.25 \text{ F} \cdot \text{g}^{-1}$ for sponge electrodes fabricated from graphene, poly(3,4-ethylenedioxythiophene) (PEDOT) and MnO_2 , with a 99% capacitance retention over 1000 stretching cycles [44].

At $0.5 \text{ A} \cdot \text{g}^{-1}$ and after 400 cycles, the specific capacitance of PTh diminished in approximately 37%, with a value of $111 \text{ F} \cdot \text{g}^{-1}$. In the case of PTh/rGO, the same test produced a decay in C of 40%, presenting a final value of $127 \text{ F} \cdot \text{g}^{-1}$. Therefore, the introduction of reduced graphene oxide to a polythiophene film by electrochemical polymerization in the above described conditions, does not increase the stability of the film after repetitive cycles of charge and discharge.

3.2. Electrochemical impedance spectroscopy (EIS) characterization

Impedance spectroscopy experiments are very useful to obtain a deeper understanding into the capacitance and other relevant electrochemical information of composite materials. Figure 5 shows the electrochemical impedance spectra for the modified electrodes with the synthesized materials.

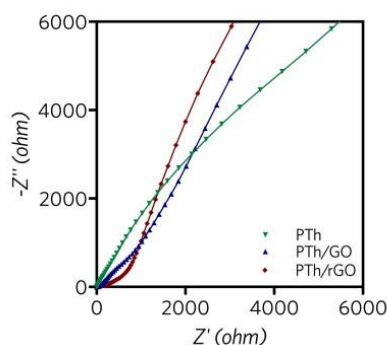


Figure 5. Nyquist plots of modified platinum electrode at open circuit potential in KCl 1 M.

Typically, the impedance analysis can be divided in high- and low-frequency regions. The high-frequency zone is related to interfacial processes, while at lower frequencies, the imaginary part of the impedance spectra is related to the capacitive behavior of the electrode, related to the charging mechanism, and in an ideal capacitor tends to a 90° vertical line. In the case of PTh modified electrode, no obvious semicircle was registered at the frequencies selected in this study, suggesting that the resistance to electron transfers can be neglected. PTh/GO and PTh/rGO modified electrodes exhibited an arc at the high-frequency zone. The larger diameter of the arc for the PTh/GO modified Pt electrode, indicates a low charge transfer rate resulting from a high electron transfer resistance. Then, the reduction of GO improves the conductive properties of the composite.

At low frequencies, the 45° -sloped region corresponds to the Warburg resistance resulting from the frequency dependence of the ion diffusion/transport in the electrolyte. At this zone, PTh/rGO showed a line closer to 90° compared to PTh/GO, suggesting a better capacitive behavior. From the EIS analysis, it can be seen that PTh/rGO exhibited a lower charge transfer resistance and a better capacitive behavior than that of the PTh. This result is consistent with the capacitance evidence. Previous reports related to the electrochemical preparation of conducting polymers and rGO composites, shown similar results. PPy/rGO composites presented better capacitive behavior than PPy/GO films [45], while the introduction of GO in PANI [46] and PEDOT [47] films by electropolymerization, resulted in composites with better performance than the sole polymer films. The reduced resistance of the composites was associated to higher surface area and to the presence of charged GO counter ions located in the vicinity of the conducting polymer matrix, which are more easily available for the charge compensation process [48]. Therefore, the lower resistance of the PTh/rGO composite could be attributed to the network of the reduced graphene structure, which facilitates the efficient access of electrolyte ions to the surface and reduces the ion diffusion path.

4. CONCLUSIONS

Graphene oxide was incorporated to a polythiophene film by electrochemical polymerization and further reduced using cyclic voltammetry. This technique is a one-step method for the preparation of composites, and unlike traditional chemical synthesis has a simple and direct protocol, with no need of polymeric binders or covalent modifications. The synthesized PTh/rGO film presented higher conductivity in comparison to its oxidized form (PTh/GO) and polythiophene. However, PTh/rGO deviated from the traditional rectangular symmetric current–potential profile and exhibited an asymmetric triangular charge-discharge shape with a non-linear potential-time relationship, indicative of a low reversibility during the charge-discharge processes and poor capability as supercapacitor material. Moreover, its stability after cycling considerably decreased. Therefore, the introduction of reduced graphene oxide to a polythiophene film in the above described conditions, does not increase the stability after repetitive cycles of charge and discharge. Based on these evidence, PTh/rGO, a systematic study considering variables like the concentration of the monomer and GO, and electrodeposition time need to be accomplished to improve the final performance and stability of the film, in order to be applied as supercapacitor material.

ACKNOWLEDGEMENTS

M.B.C. is grateful to Fondecyt for funding this research (Project Inicio 11140107).

References

1. J.-M. Tarascon and M. Armand, *Nature*, 414 (2001) 359.
2. D.J. Lipomi and Z. Bao, *Energy Environ. Sci.*, 4 (2011) 3314.
3. D. Pech, M. Brunet, P.-L. Taberna, P. Simon, N. Fabre, F. Mesnilgrete, V. Conédéra and H. Durou, *J. Power Sources*, 195 (2010) 1266.
4. C. Liu, F. Li, L.P. Ma and H.M. Cheng, *Adv. Mater.*, 22 (2010).
5. C.-W. Liew, S. Ramesh and A. Arof, *Materials & Design*, 92 (2016) 829.
6. B. Conway, *Scientific Fundamentals and Technological Applications* (1999).
7. K.-W. Nam and K.-B. Kim, *J. Electrochem. Soc.*, 149 (2002) A346.
8. S.L. Candelaria, R. Chen, Y.-H. Jeong and G. Cao, *Energy Environ. Sci.*, 5 (2012) 5619.
9. Y. Sun, Q. Wu and G. Shi, *Energy Environ. Sci.*, 4 (2011) 1113.
10. H. Zhu, X. Wang, X. Liu and X. Yang, *Adv. Mater.*, 24 (2012) 6524.
11. X. Yang, C. Cheng, Y. Wang, L. Qiu and D. Li, *Science*, 341 (2013) 534.
12. L.L. Zhang and X. Zhao, *Chem. Soc. Rev.*, 38 (2009) 2520.
13. P. Simon and Y. Gogotsi, *Acc. Chem. Res.*, 46 (2012) 1094.
14. X. Li and B. Wei, *Nano Energy*, 2 (2013) 159.
15. M.Y. Ghotbi and M. Azadfalsh, *Materials & Design*, 89 (2016) 708.
16. Y. Cui, Q.-Y. Cheng, H. Wu, Z. Wei and B.-H. Han, *Nanoscale*, 5 (2013) 8367.
17. X. Wang and G. Shi, *Energy Environ. Sci.*, 8 (2015) 790.
18. A. Voronin, F. Ivanchenko, M. Simunin, A. Shiverskiy, A. Aleksandrovsky, I. Nemtsev, Y. Fadeev, D. Karpova and S. Khartov, *Appl. Surf. Sci.*, 364 (2016) 931.
- [19. W. Quan, Z. Tang, S. Wang, Y. Hong and Z. Zhang, *Chem. Commun.*, 52 (2016) 3694.
20. J. Yan, T. Wei, B. Shao, Z. Fan, W. Qian, M. Zhang and F. Wei, *Carbon*, 48 (2010) 487.
21. Q. Wu, Y. Xu, Z. Yao, A. Liu and G. Shi, *ACS Nano*, 4 (2010) 1963.
22. A. Laforgue, P. Simon, C. Sarrazin and J.-F. Fauvarque, *J. Power Sources*, 80 (1999) 142.
23. M.R. Karim, C.J. Lee and M.S. Lee, *J. Polym. Sci., Part A: Polym. Chem.*, 44 (2006) 5283.
24. Q. Lu and Y. Zhou, *J. Power Sources*, 196 (2011) 4088.
25. J. Zhao, Y. Xie, Z. Le, J. Yu, Y. Gao, R. Zhong, Y. Qin and Y. Huang, *Synth. Met.*, 181 (2013) 110.
26. F. Alvi, M.K. Ram, P. Basnayaka, E. Stefanakos, Y. Goswami, A. Hoff and A. Kumar, *ECS Trans.*, 35 (2011) 167.
27. S.K. Yadav, R. Kumar, A.K. Sundramoorthy, R.K. Singh and C.M. Koo, *RSC Advances*, 6 (2016) 52945.
28. J. Melo, E. Schulz, C. Morales-Verdejo, S. Horswell and M. Camarada, *Int. J. Electrochem. Sci.*, 12 (2017) 2933.
29. Y. Shao, M.F. El-Kady, L.J. Wang, Q. Zhang, Y. Li, H. Wang, M.F. Mousavi and R.B. Kaner, *Chem. Soc. Rev.*, 44 (2015) 3639.
30. D. Li, M.B. Müller, S. Gilje, R.B. Kaner and G.G. Wallace, *Nat. Nanotech.*, 3 (2008) 101.
31. H.J. Shin, K.K. Kim, A. Benayad, S.M. Yoon, H.K. Park, I.S. Jung, M.H. Jin, H.K. Jeong, J.M. Kim and J.Y. Choi, *Advanced Functional Materials*, 19 (2009) 1987.
32. G.K. Ramesha and S. Sampath, *J. Phys. Chem. C*, 113 (2009) 7985.
33. A. Viinikanoja, Z. Wang, J. Kauppila and C. Kvarnström, *Physical Chemistry Chemical Physics*, 14 (2012) 14003.
34. W.S. Hummers and R.E. Offeman, *J. Am. Chem. Soc.*, 80 (1958) 1339.
35. M.M. Gvozdenović, B.Z. Jugović, J.S. Stevanović and B.N. Grgur, *Hemijaska industrija*, 68

- (2014) 673.
36. F. Beck and U. Barsch, *Macromol. Chem. Phys.*, 194 (1993) 2725.
 37. R. Schrebler, P. Grez, P. Cury, C. Veas, M. Merino, H. Gómez, R. Córdova and M.A. del Valle, *J. Electroanal. Chem.*, 430 (1997) 77.
 38. Z. Wang, X. Zhou, J. Zhang, F. Boey and H. Zhang, *J. Phys. Chem. C*, 113 (2009) 14071.
 39. J. Zhang, J. Ma, L.L. Zhang, P. Guo, J. Jiang and X.S. Zhao, *J. Phys. Chem. C*, 114 (2010) 13608.
 40. J. Zhang, J. Jiang and X.S. Zhao, *J. Phys. Chem. C*, 115 (2011) 6448.
 41. B. You, L. Wang, L. Yao and J. Yang, *Chem. Commun.*, 49 (2013) 5016.
 42. K. Zhang, B.T. Ang, L.L. Zhang, X.S. Zhao and J. Wu, *J. Mater. Chem.*, 21 (2011) 2663.
 43. A. Alabadi, S. Razzaque, Z. Dong, W. Wang and B. Tan, *J. Power Sources*, 306 (2016) 241.
 44. M. Moussa, G. Shi, H. Wu, Z. Zhao, N.H. Voelcker, D. Losic and J. Ma, *Materials & Design*, 125 (2017) 1.
 45. H.-H. Chang, C.-K. Chang, Y.-C. Tsai and C.-S. Liao, *Carbon*, 50 (2012) 2331.
 46. T. Lindfors and R.-M. Latonen, *Carbon*, 69 (2014) 122.
 47. W. Si, W. Lei, Y. Zhang, M. Xia, F. Wang and Q. Hao, *Electrochim. Acta*, 85 (2012) 295.
 48. Q. Zhang, Y. Li, Y. Feng and W. Feng, *Electrochim. Acta*, 90 (2013) 95.

© 2017 The Authors. Published by ESG (www.electrochemsci.org). This article is an open access article distributed under the terms and conditions of the Creative Commons Attribution license (<http://creativecommons.org/licenses/by/4.0/>).